REPORT DOCUMENTATION PAGE

Form Approved
OMB No. 0704-0188

1. REPORT DATE *(DD-MM-YYYY)*	2. REPORT TYPE	3. DATES COVERED *(From - To)*
29-05-2008	Final Report	01 Oct 2003 - 30 Sept 2006

4. TITLE AND SUBTITLE

Analysis of TODWL PBL Wind Profiles Over Monterey Bay:
Towards ground truth winds for WindSAT and other remote sensors

5a. CONTRACT NUMBER

5b. GRANT NUMBER

N00173-03-1-G021

5c. PROGRAM ELEMENT NUMBER

6. AUTHOR(S)

Ralph C. Foster
Robert A. Brown

5d. PROJECT NUMBER

5e. TASK NUMBER

5f. WORK UNIT NUMBER

7. PERFORMING ORGANIZATION NAME(S) AND ADDRESS(ES)

Applied Physics Laboratory - University of Washington
1013 NE 40th Street
Seattle, WA 98105-6698

8. PERFORMING ORGANIZATION REPORT NUMBER

9. SPONSORING/MONITORING AGENCY NAME(S) AND ADDRESS(ES)

Naval Research Laboratory
4555 Overlook Ave SW
Washington, DC 20375

10. SPONSOR/MONITOR'S ACRONYM(S)

NRL

11. SPONSOR/MONITOR'S REPORT NUMBER(S)

12. DISTRIBUTION/AVAILABILITY STATEMENT

Unlimited

13. SUPPLEMENTARY NOTES

None

14. ABSTRACT

Under this project we analyzed data from the TOWDL (Test of Wind Doppler Lidar) data acquired from February-March, 2002 and February, 2003 over and near Monterey Bay, CA to characterize the coherent structures and to compare them to our simple models of PBL roll vortices. This information is crucial for developing Cal/Val strategies and will help advance our fundamental understanding of the planetary boundary layer (PBL). A good model of the inhomogeneous flow at the proper footprint scales is essential to correct interpretation of surface comparison data. In many cases the inherent variability in Cal/Val may be in the natural turbulent and coherent structure nature of the winds rather than in the sensor signal. Since the satellite surface wind sensors appear to detect surface stress rather than surface wind, the variability in the surface stress, which is a nonlinear function of the surface wind, must be understood.

15. SUBJECT TERMS

TODWL, Twin Otter Doppler Wind Lidar, Marine boundary layer, coherent structures, planetary boundary layers, roll vortices, organized large eddies, WindSAT

16. SECURITY CLASSIFICATION OF:			17. LIMITATION OF ABSTRACT	18. NUMBER OF PAGES	19a. NAME OF RESPONSIBLE PERSON
a. REPORT	b. ABSTRACT	c. THIS PAGE			Ralph C. Foster
U	U	U	UU		19b. TELEPHONE NUMBER *(Include area code)* 206 685-5201

Analysis of TODWL PBL Wind Profiles Over Monterey Bay: Towards ground truth winds for WindSAT and other remote sensors

Final Report: N00173-03-1-G021

PI: Ralph C. Foster,
Applied Physics Laboratory
University of Washington
1013 NE 40th St.
Seattle, WA, 98105-6698

Co-PI: Robert A. Brown,
Department of Atmospheric Sciences
Box: 351640
University of Washington
Seattle, WA. 98195-1640

1) Introduction

An imperative for calibration and validation (Cal/Val) of surface wind vector remote sensing products such as WindSAT is a characterization of the actual surface wind, its connection to the wind profile within the boundary layer and its variability (both speed and direction) over ~25 km^2 footprints. Establishing the proper ground truth wind requires accounting for the organization of the PBL turbulence by coherent structures such as longitudinal roll vortices. These km-scale rolls induce horizontal inhomogeneity in both speed and direction which affects the interpretation of point validation winds from buoys or numerical model analyzed surface winds fields.

In support of this effort, the Integrated Program Office sponsored the development and deployment of a 2-micron coherent Doppler wind lidar (DWL) profiling system on the NRL Twin Otter. The DWL included a two-axis scanner and was used to directly measure the wind profiles within the planetary boundary layer (PBL) with 100 m range gates. Routinely during field programs, the DWL winds were strongly modulated by km-scale coherent structures.

We analyzed data from the TOWDL (Test of Wind Doppler Lidar) data acquired from February-March, 2002 and February, 2003 over and near Monterey Bay, CA to characterize the coherent structures and to compare them to our simple models of PBL roll vortices. This information is crucial for developing Cal/Val strategies and will help advance our fundamental understanding of the PBL. A good model of the inhomogeneous flow at the proper footprint scales is essential to correct interpretation of surface comparison data. In many cases the inherent variability in Cal/Val may be in the natural turbulent and coherent structure nature of the winds rather than in the sensor signal. Since the satellite surface wind sensors appear to detect surface stress rather than surface wind, the variability in the surface stress, which is a nonlinear function of the surface wind, must be understood.

Many surface wind Cal/Val analyses are predicated on the myth that PBL flow is homogeneous on scales from meters to 100-km. Our theoretical and data analyses show

this is not true; in fact the PBL over the ocean generally contains embedded organized large eddies (OLE) on several scales (Brown 1980; Etling and Brown, 1993; Foster, 1996; Foster, 1997; Foster et al., 2007; Drobinski et al., 1998; Drobinski and Foster, 2003; Drobinski et al., 2006; Young et al., 2002). We have previously used detected the signature of roll vortices in lidar winds (Drobinski, et al., 1998). Our goal was to understand the inhomogeneities of the PBL flow that are induced by coherent structures since these effects impact any comparisons of buoy surface winds with satellite wind products. The practical goal for the IPO was to establish a theoretical verification for TOWDL observations of non-homogeneous data in the PBL. The current DWL observational data resolve these eddies, and comparing these data to the theory yields information on both the PBL flow and the theory that is important for WindSAT Cal/Val.

2) Data sources

2.1) DWL on Twin Otter

The primary data was collected on the NRL Twin Otter aircraft. This plane flies at 50-60 m/s at 15 to 5000 m altitude. The key instrument is a side-mounted two-micron coherent Doppler Wind Lidar (DWL) with a two-axis scanner that scans +/- 120° from horizontal and 60° in azimuth. The DWL can retrieve Line of sight (LOS) velocities with horizontal resolution of 1 to 10 m. The range gates are about 100 m wide. Scanning mode allows wind direction and speed retrievals. In addition, the aircraft was outfitted with GPS dropsondes, turbulence probes and temperature and humidity sensors. The aircraft has two independent navigation systems to locate the aircraft accurately. The lidar winds were processed at Simpson Weather Associates by G. David Emmitt and Chris O'Handley and provided to us.

2.2) Theoretical Models for Rolls

Rolls are caused by a mixed convective/shear instability of the mean flow in the PBL. Flow instabilities are initially controlled by linear dynamics and usually grow exponentially in time[1] until it reaches a point where nonlinear effects become important. The initial linear instability is symmetric – the positive and negative components of the perturbation flow are equal in magnitude. In the linear phase, the growth rate is the net imbalance between the rate at which the roll fluxes (buoyancy and momentum) extract energy from the mean flow and the rate at which energy is dissipated. At some point in the exponential growth phase nonlinear effects come into play. Usually the nonlinear effects accelerate the growth by increasing the production rates. In this case the instability reaches an amplitude where it breaks down and generates a burst of turbulence. However, as discussed in Foster (2005) PBL rolls are a form of cross-flow instability; i.e. they are associated with an inflection point in the cross-mean-flow component of the veering mean flow profile. The nonlinearities in such problems tend to modify both the roll structure and the mean flow in such a manner that the perturbation energy production rates are reduced to a point where the net ("linear" + "nonlinear") production can be

---

[1] Although Foster (1997) describes "faster-than-exponential" transient, small-scale PBL perturbations.

balanced by the dissipation. In this way a stable equilibrium is formed that consists of a modified mean flow profile with an embedded secondary circulation. The secondary circulation is similar to the original linear instability, but its shape has been modified by the nonlinear dynamics. The mean wind and buoyancy profiles are also modified in the presence of finite amplitude rolls.

The roll wavelength and orientation relative to the mean flow are both determined by the linear instability. Typical shear instabilities in unidirectional flow form roll instabilities that are aligned perpendicular to the mean flow. However, because roll instabilities are associated with the cross-wind inflection point, they tend to align more closely with the mean wind. The fastest growing PBL instabilities align at a small angle (roughly 0^{o} to 15^{o}) to the mean PBL wind direction. This angle tends to decrease as the PBL becomes more unstably stratified. Over the ocean the PBL is generally nearly-neutrally to moderately unstably stratified. The wavelength of the rolls tends to select wavelengths for which the upper branch of the over-turning circulation is near the top of the PBL.

The first simple nonlinear model for roll vortices was developed by Brown (1970; 1972). It assumes a 2-D (cross-wind and vertical) symmetric overturning circulation coupled with a temperature perturbation. It is based on a linear instability of the PBL mean flow. Nonlinear effects are included by assuming that the roll has exactly the same symmetric shape as the linear instability, but has a finite amplitude that is determined by a negative feedback of the shear production terms back into the mean flow. A scale analysis (Foster, 1996) shows that these assumptions leave out two equally important nonlinear effects, which are the generation of slaved harmonic modes and the interactions and self interactions between the fundamental mode and the harmonics.

Foster (1996) developed a more complete simple nonlinear model for roll vortices that includes all three velocity components (along-wind, cross-wind and vertical) and the buoyancy perturbations. This model uses a high-order expansion that includes the shear production feedback for the fundamental and the slaved harmonics, the generation of slaved harmonics and the interactions and self interactions between the fundamental and the harmonics. This model accurately captures the asymmetry in the roll circulations in which the updrafts are narrower and stronger than the downdrafts. The asymmetry increases with increasingly unstable stratification. Associated with the asymmetry is an along-wind modification that is much stronger in the convergent region below the updraft branch of the overturning (cross-roll and vertical) circulation than in the divergent layer below the downdraft branches. While the overturning compnents of the roll circulation span the depth of the PBL, the along-wind modifications are trapped near the surface. This has important implications for the effects of rolls on the surface stress. The implication of the roll asymmetry is that, while rolls modify the surface stress in both the upward and downward branches of the circulation, the roll modification due to ejections of slower-moving near-surface air is stronger than the downward sweeps of faster-moving air from higher in the PBL.

Figure 1 sketches the general sense of the roll circulation. This is the coherent, quasi-steady perturbation flow that must be added to the generally homogeneous mean flow in typical conditions. The total PBL flow is the sum of the mean + perturbation +

turbulence. Note that the strength of the along-wind perturbation is in the neighborhood of 3 to 7 times stronger than that of the overturning circulation. Because of this and because the along-wind component of the mean flow is stronger and has higher shear, the along-roll shear production is much greater than that of the across-roll shear production – even though the basic instability is associated with the cross-flow inflection point.

To understand the following analysis, it is important to visualize how line-of-sight velocity (VLOS) lidar will sample the roll structure. Consider a level flight leg with the lidar in a foreword stare mode, which is the common configuration for the data discussed here. The VLOS will capture the components of the rolls (plus total wind) that projects into the line of sight. When the plane is flying roughly along the mean wind, the sampled roll component will be dominated by the along wind perturbations. However, since the along-wind perturbation is trapped near the surface, only a weak signal will be detected unless the plane is flying near the surface. For across-wind flight legs, most of the near-surface, along-roll perturbations will be nearly orthogonal to the lidar beam and contribute little to VLOS. In this case the VLOS will be dominated by the weaker cross-roll contribution to the overturning circulation. This component is strongest near the surface, weak in the middle of the PBL and stronger again, but not as strong as the near-surface layer, near the top of the PBL.

Because of the small angle between the rolls and the mean wind, along- and across-wind flight legs will cut through the rolls at an angle. The aliased wavelength is $\lambda_{LOS} = \lambda / \sin(\psi)$ where ψ is the angle between the LOS and the rolls. For the across-wind flight legs, the aliasing of rolls wavelength is small. However, in the along-wind direction, the aliasing is large and very sensitive to small changes in ψ. Figure 2 shows typical aliased wavelengths for the conditions of this study.

The roll model was used to predict the wavelength, orientation, vertical profiles and strength of the roll vortices for the conditions of the DWL acquisitions. A module was built that flew a virtual Twin Otter through the roll solution using the navigation and beam pointing data from the Twin Otter flight legs. The roll solution was sampled in a manner consistent with that of the DWL for comparison with the DWL data.

3) Analysis

We focused on TOWDL data acquired on 20 February 2003. The mean wind was approximately from the NNW (320°) with a strength of ~ 16 m s^{-1}. Three flight legs were dedicated to documenting the roll structure. In these flights, the lidar beam was set in a forward stare mode and the Twin Otter flew straight and level flight legs that were several minutes long. Legs 1 and 2 formed an "L" pattern approximately along and across the mean wind at 30 m above the sea surface. Leg 3 was approximately into the mean wind, but at a higher altitude of 400 m, about the mid-depth of the PBL. The legs are summarized in Table 1.

Table 1: Summary of TODWL flight legs, 20 Feb, 2003					
Leg	Time	Length (km)	Altitude (m)	Heading	Lidar Elevation Angle
1	12:35 – 12:40	16.4	30	150°	1.3°
2	12:46 – 12:49	8.9	30	58°	0.5°
3	13:27 – 13:30	10.7	400	330°	0.8°

Figure 3 shows MODIS near IR imagery of the study region for orbits near the time when the data were acquired (UTC is local time plus 8 hours). Included on the Figure are the three flight legs to be discussed. At the time of the flight, only very wispy clouds could be seen. This is confirmed in the MODIS imagery in which thin cloud streets (note the low radiances) form farther off-shore than the three flight legs. From these images we estimated that the PBL depth was ~800 m and the wavelength of the cloud streets was about 1700 to 2000 m.

A common misconception is that cloud streets are a reliable indicator of the presence or absence of PBL roll vortices. However, cloud streets only form in the updraft branches of the roll circulation when the thermodynamics are favorable. So, while the presence of PBL cloud streets is almost always associated with rolls, the absence of cloud streets does not mean that rolls have not formed. In fact, over several years of DWL measurements in and around Monterey, including many flight hours over land during day and night, roll vortices are nearly always present (G. D. Emmitt, *pers. comm.*). Hence, we used these estimates of the roll characteristics in a region very near the flights as part of the validation of our results.

As discussed above, the 30 m flight legs should detect the strongest roll signature. In order to aid in the visualization of the VLOS that will be analyzed more completely below, Figure 4 maps the gate height and VLOS for Legs 1 and 2. For both legs, the plotted VLOS is the deviation from the mean VLOS along that flight leg (covering all gates). Note that the lidar elevation angle was higher in Leg 1 than in Leg 2, so the VLOS at the farthest ranges are from higher in the PBL in Leg 1 (~170 m) than in Leg 2 (~85 m) on average. The aircraft pitch induced a strong modulation of the elevation angle during the flight in both legs. Consequently, some of the far range returns are actually from much higher or lower in the PBL than the average. (When the pitch pointed the beam downwards, some of the far range returns are from the sea surface.). In the cross-wind Leg 2, the periodic modulation (wavelength of about 2 km) of the mean wind by roll vortices is readily apparent. Leg1 appears to cut through about 3 rolls and the aliasing of the wavelength is clear. While mapped plots such as Figure 4 are useful for 3-D visualization of the lidar returns, it is difficult to make quantitative analyses.

Figure 5a re-plots the along-wind Leg 1 VLOS data in Figure 4 for each range as a function of along-flight-track distance. The mean of -14.9 m s^{-1} has been subtracted to emphasize the coherent structures. Each vertical stripe of wind returns in Figure 5 corresponds to one of forward-projecting stripes from Figure 4. The near-range returns come from about 500 m down-track from the plane and the farthest returns are from

about 6 km down-track. The mean elevation as a function of range is shown on the right hand axis. The vertical stripes of locally much higher or weaker VLOS than nearby points correlate with aircraft pitch pointing the beam either down towards the sea surface or much higher in the PBL. The backwards slope of the periodic modulation is due to the lidar beam sampling the same structure as the plane approaches it. The largest scale structure evident in this plot has a wavelength of about 8 km, which suggests that the Twin Otter was flying at about a 14° angle relative to the rolls, which is consistent with a nearly-neutral boundary layer. This is consistent with the relatively high winds (~15 m s^{-1}) and weak or absent cloud cover in the MODIS imagery.

Figure 5b presents the predicted lidar returns from the roll theory assuming a constant elevation angle, constant flight altitude of 30 m and using the aircraft heading. The correspondence in both magnitude and structure between the theory and observations is quite striking. Rolls are accounting for a ~+/- 4 m s^{-1} perturbation of the VLOS around a mean of ~15 m s^{-1}. Of particular interest to the IPO for WindSAT Cal/Val is how these perturbations will affect the surface winds. We use the roll model and standard Monin-Obukhov similarity to reduce the VLOS perturbations to the sea surface. The result is shown in Figure 6. The neutral equivalent wind at 10 m, U_{10}^{N}, has a mean of about 14.7 m s^{-1}, but, due to the rolls alone, ranges between 12.5 to 16.5 m s^{-1} over down wind distances of ~8 km, (or cross-wind distances of about 2 km). This is a vitally important aspect of sub-WindSAT footprint variability in surface stress that must be considered in the construction of geophysical model functions for wind retrievals from microwave emission and in the Cal/Val of the WindSAT data.

Referring back to Figure 5a, note the presence of much smaller wavelength periodic modulations of comparable magnitude to that of the rolls in the near ranges. The aliased wavelength is about 500 m. They are strongest when the mean gate height is less than about 100 m. These are very suggestive of near-surface streaks such as are described in Foster (1997); Drobinski and Foster (2003); Drobinski et al. (2004) and Foster et al. (2007). Future studies ought to focus some resources on these structures since Foster et al. (2007) suggest that they play a key role in the maintenance of the surface stress.

We now turn to the cross-wind low-level flight Leg 2 (Figure 7). The periodic roll modulation is clear. In this case we have subtracted a mean of 5.3 m s^{-1}, which has likely not fully accounted for asymmetry between positive and negative velocity perturbations. However, the 2 km roll wavelength is apparent in the data and matches well with the theory. Note that as discussed above, and consistent with the theoretical prediction, the primarily cross-wind roll perturbations are much weaker than the along-wind roll perturbations seen in Leg 1. Consequently, the cross-wind legs are best for detecting rolls and characterizing their wavelength. However, long down-wind (or perhaps better, long oblique) flight legs are best for characterizing their effect on the surface stress.

Leg 3 was a short into-wind leg relatively high in the boundary layer (Figure 8). At these heights, the magnitude of the along-wind roll perturbation is much smaller than near the surface and the length of 10 km is too short for a detailed study. Comparison with the theoretical model shows that the general shape and magnitude of the

perturbation is still consistent with the theory. However, we cannot draw any firm conclusions.

4) Summary

We analyzed Doppler wind lidar data acquired during the TOWDL experiments over Monterey Bay in 2003 and extracted the signature of coherent roll vortices. We find that our simple nonlinear theories for PBL roll vortices agree quite well with the observations. Of particular note are the agreement between theory and data of: (1) wavelength and orientation of the rolls relative to the mean wind; (2) strength of the along-wind and across-wind roll perturbation velocities; (3) confirmation of the theoretical prediction that the along-wind velocity perturbation is the strongest component of the roll flow and is trapped near the surface. We also analyzed the effects of rolls on the surface wind speed, which is a necessary aspect of Cal/Val of satellite surface wind sensors such as WindSAT. We find that rolls alone account for periodic peak-to-peak modulations of the surface wind speed, U_{10}^{N}, of 4 m s^{-1} (mean of ~15 m s^{-1}) over downwind distances of ~8 km or crosswind distance of ~2 km. This *natural* variability must be understood and well characterized in all Cal/Val efforts. And, since stress is a nonlinear function of surface wind speed, and since satellite remote sensors appear to detect stress as opposed to wind, this effect must be accounted for in the construction of geophysical model functions and Cal/Val of sensors such as WindSAT.

5) Presentations

G.D. Emmitt, C. O'Handley, R.C. Foster, RA Brown, 2002: Using an Airborne Doppler Lidar to Evaluate QuikSCAT and RadarSat Derived Winds, Eos Trans. AGU, 83(47), Fall Meet. Suppl., Abstract OS72A-0348, 2002

Foster, RC, RA Brown, GD Emmitt, C O'Handley, 2004: Using TOWDL data to validate marine boundary layer models, AMS 15th Conference on Air-Sea Interaction, 9-14 Aug, 2004, Portland ME.

Emmitt, GD; and C. O'Handley, S. Greco, R. Foster, and R. A. Brown, 2005: Airborne Doppler Wind Lidar Investigations of OLEs over the Eastern Pacific and the Implications for Flux Parameterizations, 6th Conference on Coastal Atmospheric and Oceanic Prediction and Processes

Foster, R C, 2006: The Role of Unparameterized Boundary Layer Processes on Tropical Cyclone Intensity Prediction, Eos Trans. AGU, 87(52), Fall Meet. Suppl., Abstract A13E-0991.

Foster, RC and RA Brown: 2004: Analysis of TOWDL PBL Winds: Towards Ground Truth for WindSAT & Other Remote Sensors, NPOESS IGS Review, Silver Spring, MD, 3 March, 2004.

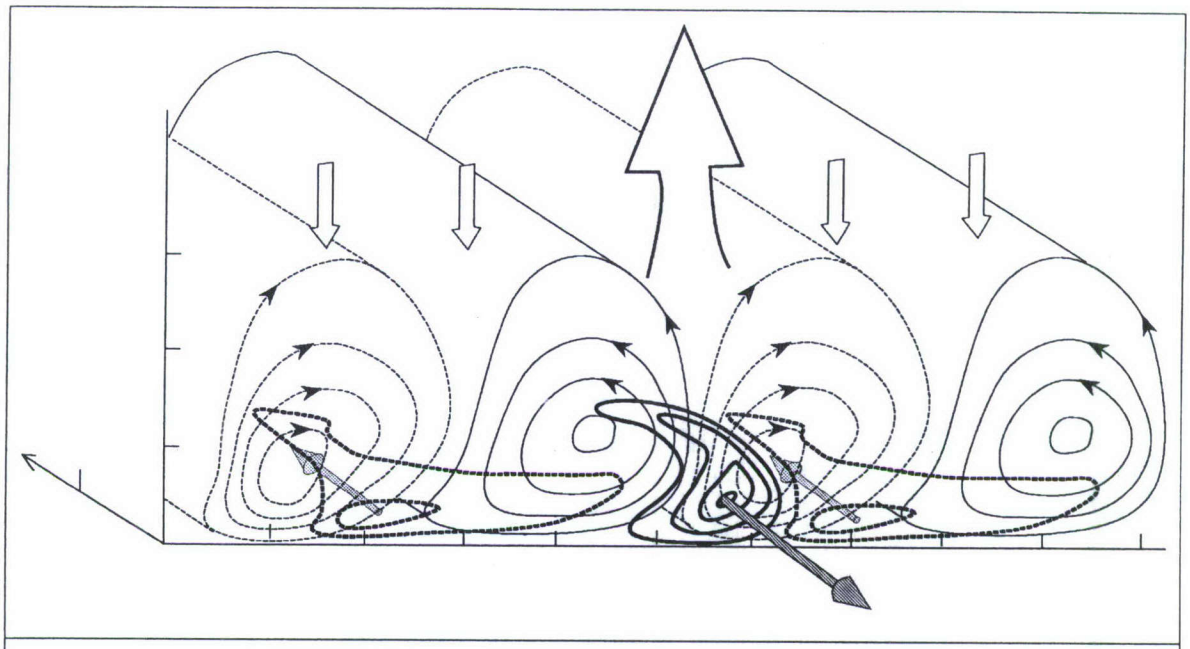

Figure 1: Schematic of typical roll circulation. Mean flow is into the page. Near-surface contours show the along roll (roughly along-wind) velocity perturbation. Large-scale contours show the stream function of the overturning circulation. .

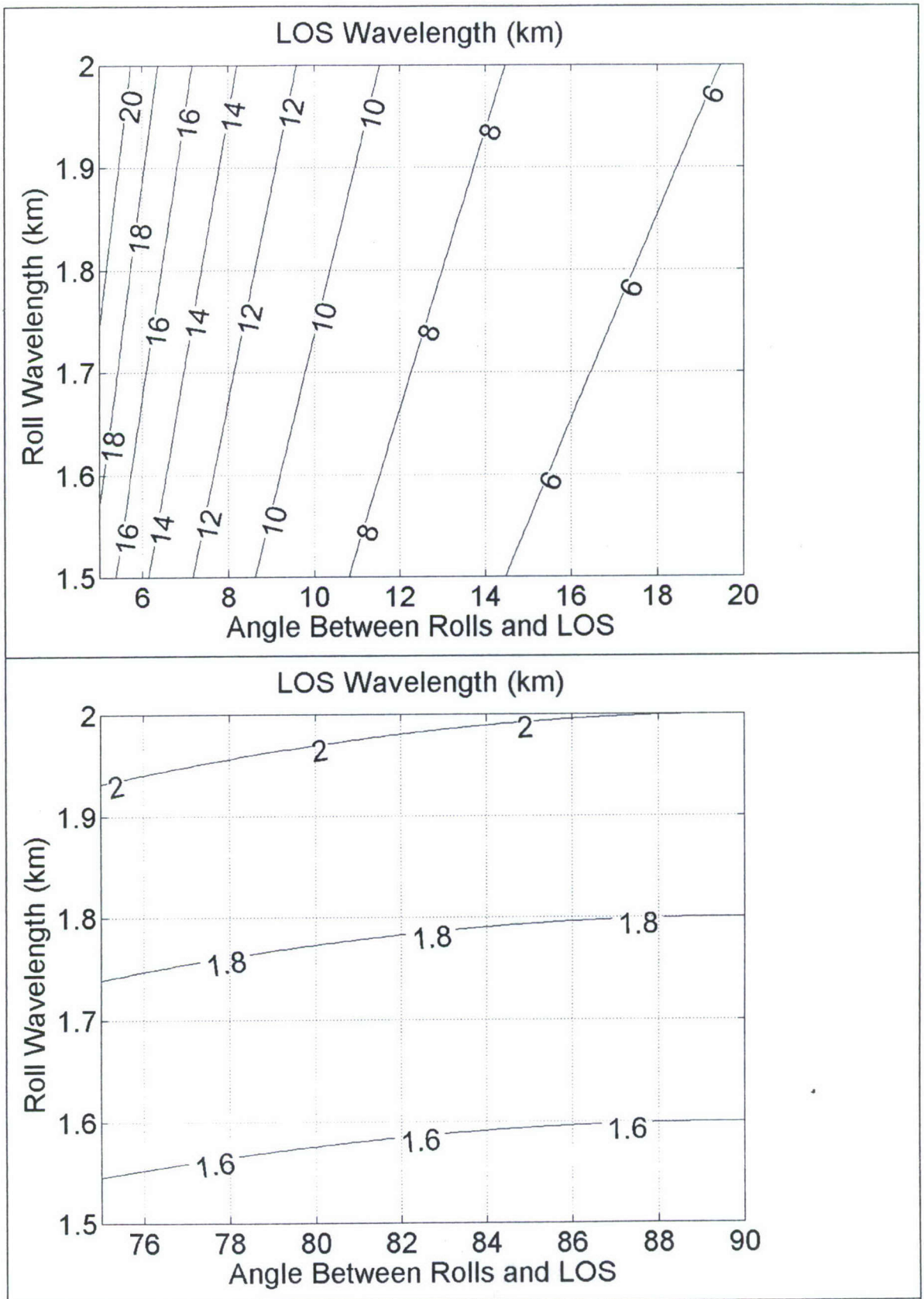

Figure 2: LOS aliasing of roll wavelengths. (a) Along-wind; (b) Across-wind.

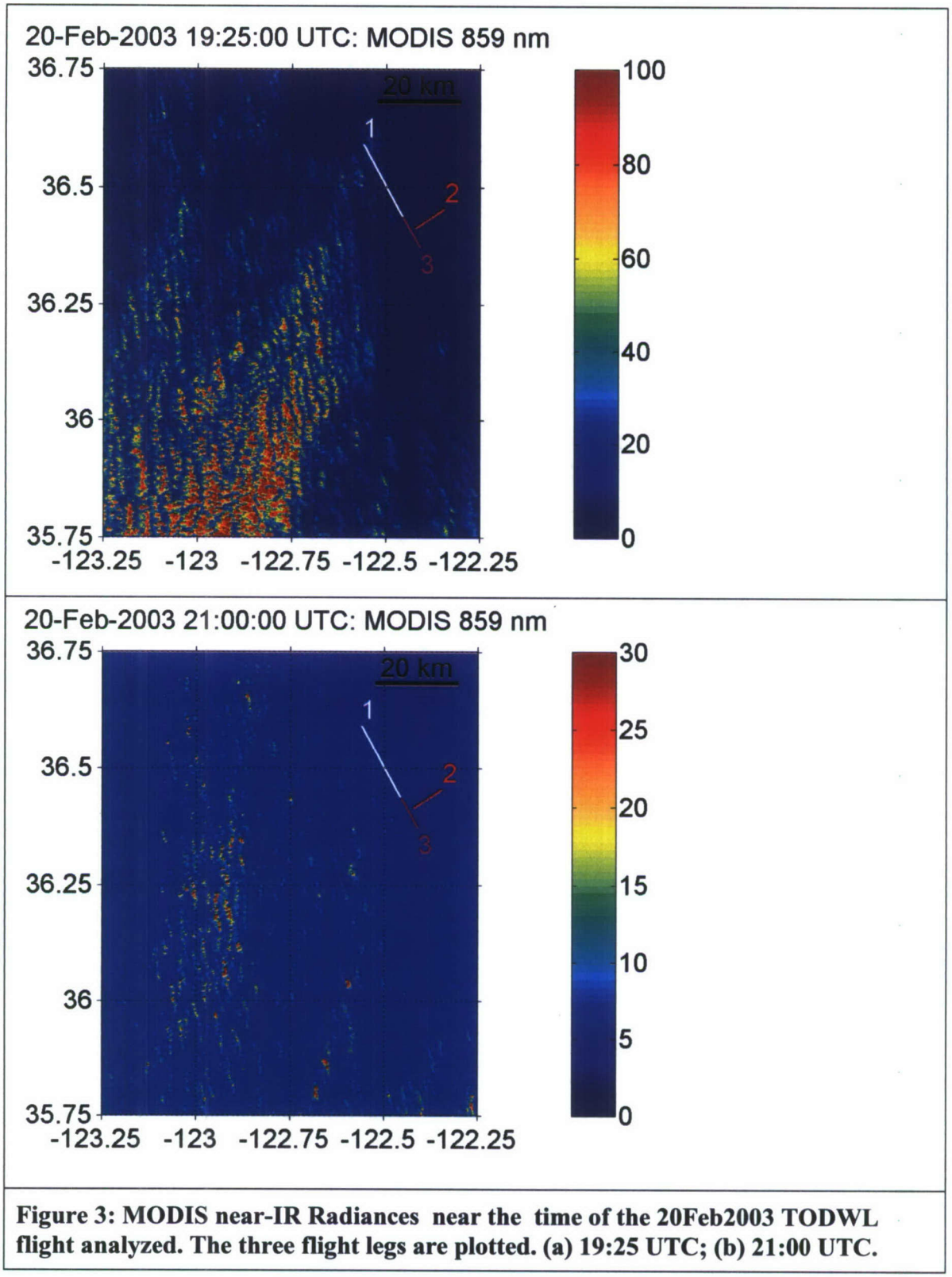

Figure 3: MODIS near-IR Radiances near the time of the 20Feb2003 TODWL flight analyzed. The three flight legs are plotted. (a) 19:25 UTC; (b) 21:00 UTC.

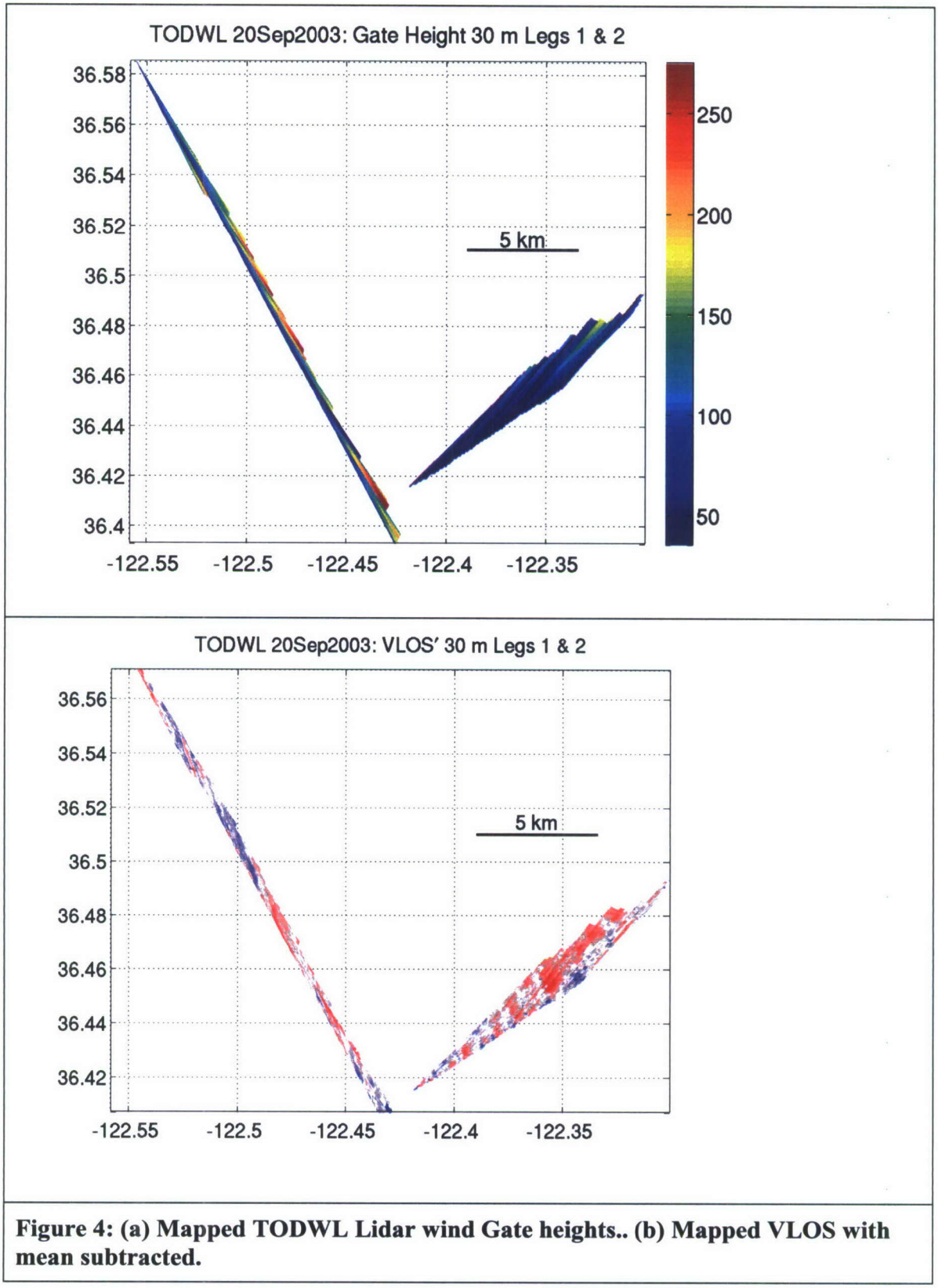

Figure 4: (a) Mapped TODWL Lidar wind Gate heights.. (b) Mapped VLOS with mean subtracted.

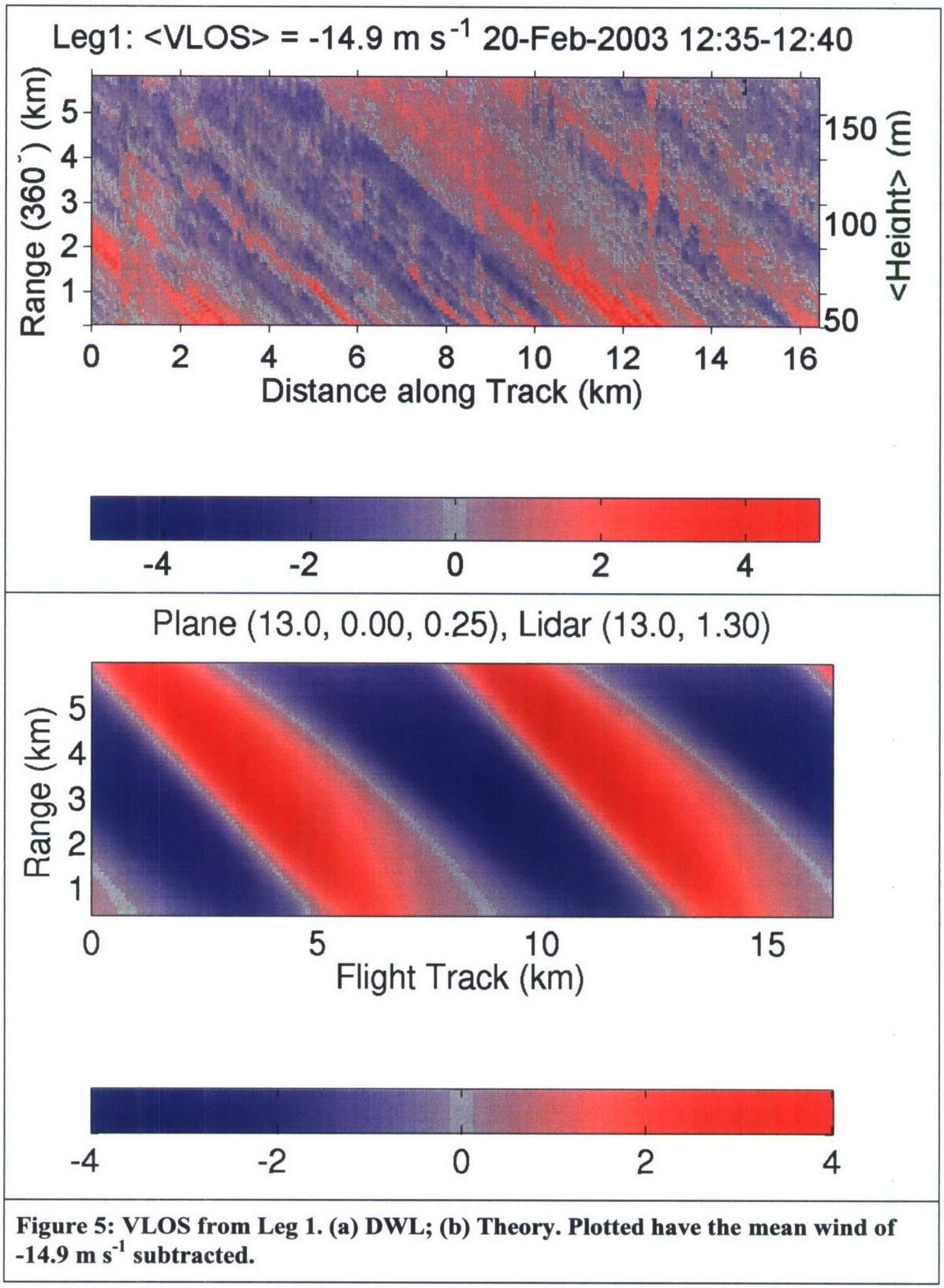

Figure 5: VLOS from Leg 1. (a) DWL; (b) Theory. Plotted have the mean wind of -14.9 m s^{-1} subtracted.

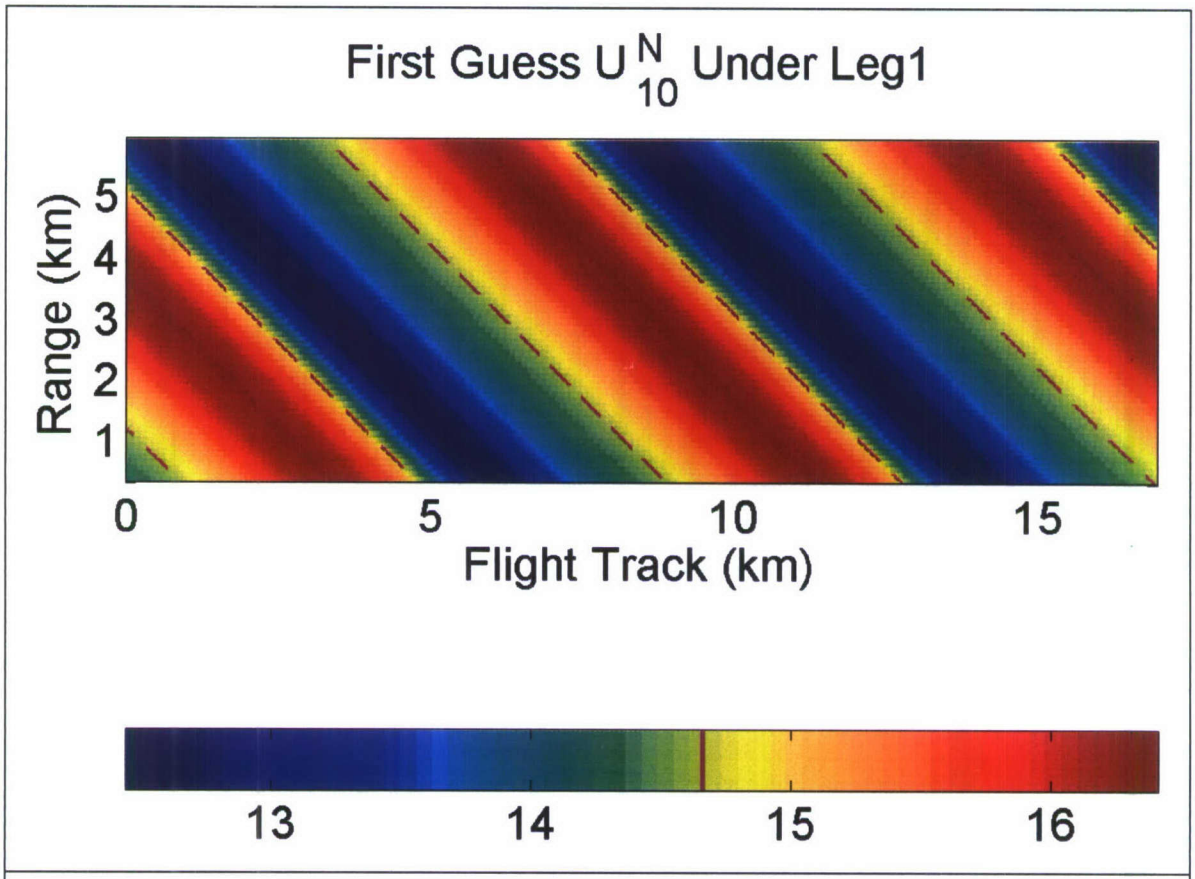

Figure 6: Surface wind estimated from roll theory and Monin-Obukhov similarity.

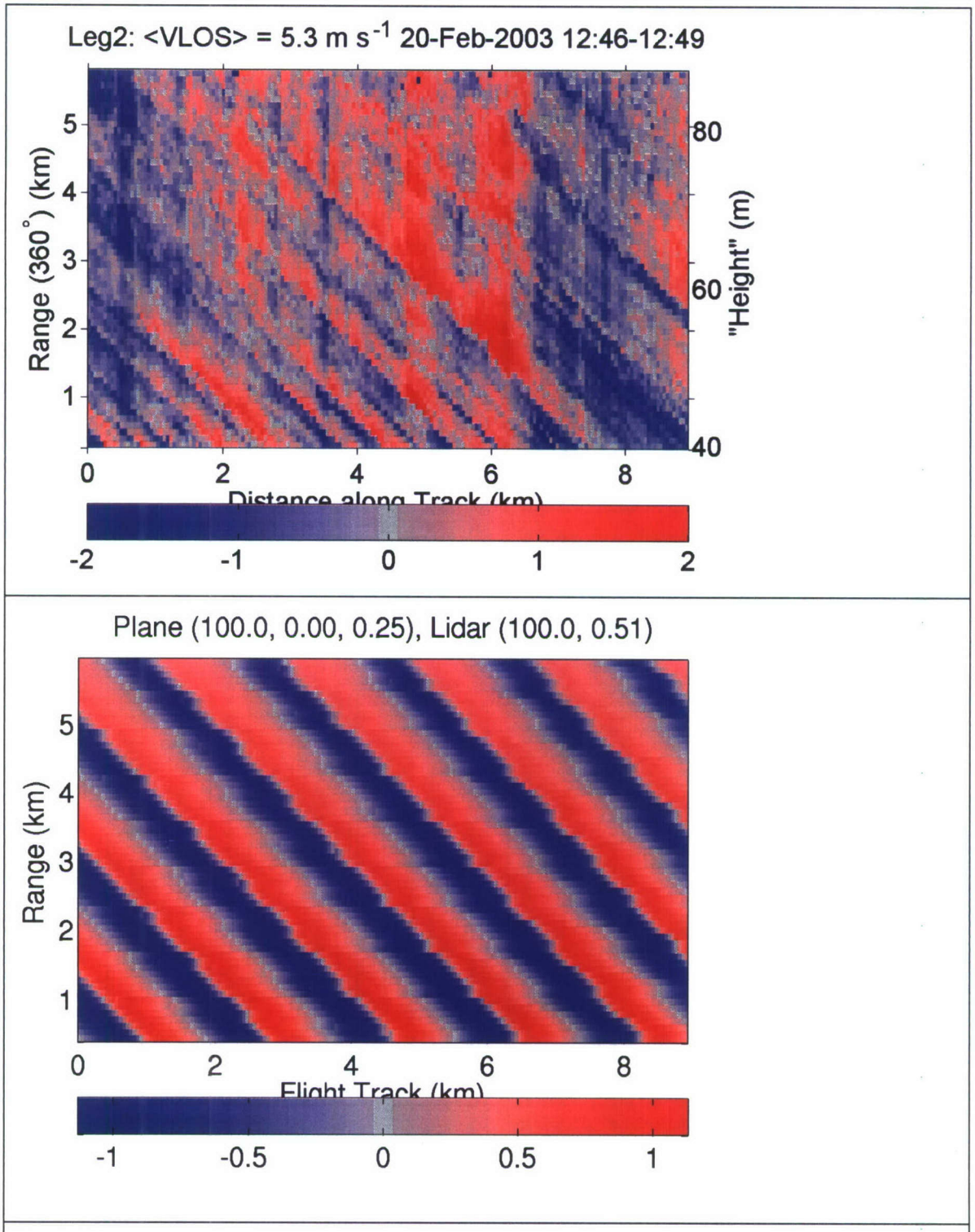

FIGURE 7: VLOS from Leg 2. (a) DWL; (b) Theory. Plotted have the mean wind of 5.3 m s^{-1} subtracted

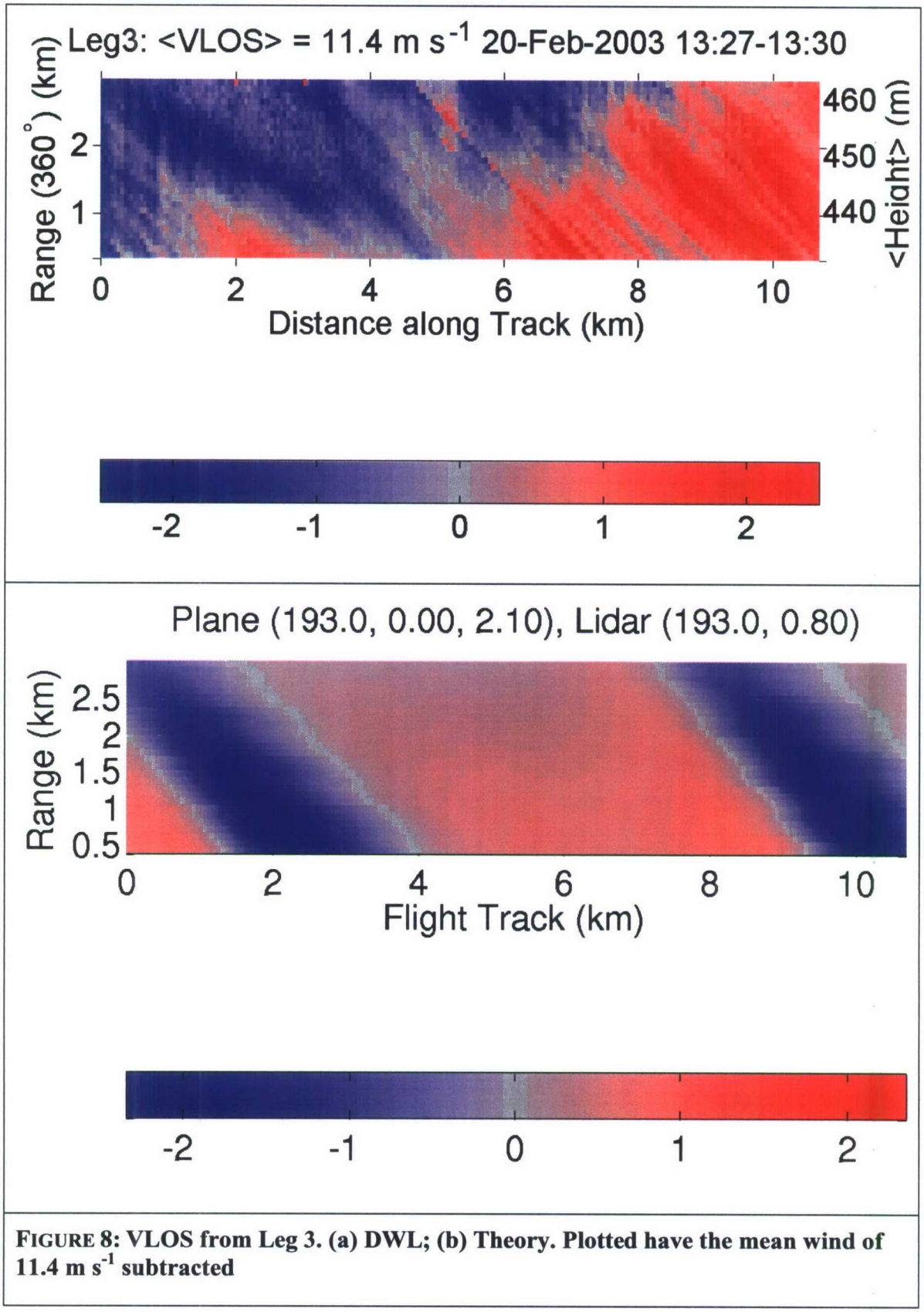

FIGURE 8: VLOS from Leg 3. (a) DWL; (b) Theory. Plotted have the mean wind of 11.4 m s^{-1} subtracted

6) References:

Brown, RA 1970: A secondary flow model for the planetary boundary layer. *J. Atmos. Sci.*, **27**, 742-757.

Brown, RA 1972: On the inflection point instability of a stratified Ekman boundary layer. *J. Atmos. Sci.*, **29**, 850–859.

Brown, RA 1980: Longitudinal instabilities and secondary flows in the planetary boundary layer. *Rev. Geophys. Space Phys.*, **18**, 683–697.

Drobinski, P, R.A. Brown, P.H. Flamant, J. Pelon, 1998: Evidence of Organized Large Eddies by Ground-Based Doppler Lidar, Sonic Anemometer and Sodar, *Bound.-Layer Meteor.*, **88**, 343-361.

Drobinski P, and R.C. Foster, 2003: On the origin of near-surface streaks in the neutrally-stratified planetary boundary layer. *Bound.-Layer Meteor.*, **108**, 247–256.

Drobinski, P, P. Carlotti, R.K. Newsom, R.M Banta, R.C. Foster and J-L Redelsberger, 2004: The structure of the near-neutral atmospheric surface layer, *J. Atmos. Sci*, **61**, 699-714.

Etling, D., RA Brown, 1993: A Review of Large-Eddy dynamics in the Planetery Boundary Layer, *Bound.-Layer Meteor.*, **65**, 215-248.

Foster, RC 1996: An analytic model for planetary boundary layer roll vortices, PhD thesis, University of Washington, 193 pp.

Foster, RC, 1997: Structure and Evolution of Optimal Ekman Layer Perturbations, *J. Fluid Mech.*, **333**, 97-123.

Foster, RC and G. Levy, 1998: The contribution of organized roll vortices to the surface wind vector in baroclinic conditions, *J. Atmos. Sci*, **55**, 1466-1472.

Foster, RC, RA Brown, A. Enloe, Baroclinic modification of midlatitude surface wind vectors observed by the NASA scatterometer, *J. Geophys. Res.*, **104(D24),** 31225-31237.

Foster RC, 2005: Why rolls are prevalent in the hurricane boundary layer, *J. Atmos. Sci.* **62** 2647-2661.

Foster R.C., Vianey F., Drobinski P., Carlotti P, 2006: Near-Surface Sweeps and Ejections in a Neutrally-Stratified Large Eddy Simulation. *Bound.-Lay Meteor.*, 120, 229-255.

Young, G, DA Kristovich, M Hjelmfelt, R.C. Foster, 2002: Rolls, Streets, Waves, and More: A Review of Quasi-Two-Dimensional Structures in the Atmospheric Boundary Layer, *Bull. Amer. Meteor. Soc.*, **83**, 997-1001. (Details in electronic supplement available at AMS website.)